

Vacuum-Enhanced Recovery of Water and NAPL: Concept and Field Test

Ralph S. Baker and John Bierschenk

ENSR Consulting and Engineering, Acton, MA 01720

ABSTRACT: Many hydrocarbon-contaminated soils contain nonaqueous phase liquid (NAPL) following releases from facilities such as underground storage tanks and pipelines. The recovery of free product by pumping from extraction wells or trenches is often an essential prerequisite step prior to further remedial actions. Vacuum-enhanced NAPL recovery (sometimes referred to as dual-phase extraction or bioslurping) has attracted recent attention because it offers a means to increase NAPL recovery rates compared with conventional methods, and to accomplish dewatering, while also facilitating vapor-based unsaturated zone cleanup. A conceptual model is presented that recognizes the effects that vacuum-enhanced recovery has on soil water and NAPL, with a focus on liquid residing at negative gage pressures and therefore lacking sufficient potential energy to flow into a conventional recovery well or trench. The imposition during vacuum-enhanced recovery of subatmospheric pressures within the subsurface can reduce the required potential energy (i.e., the entry suction), allowing liquid to be extracted that hitherto had not been able to flow into the well; moreover, it induces both pneumatic and hydraulic gradients toward the vacuum source that increase the rate of water and NAPL recovery. This conceptual model was tested during a 3-week-long pilot study at a South Carolina industrial site at which diesel fuel had been discovered in a saprolite formation. During Phase 1 of the pilot study, conventional recovery (liquid only) was carried out from a well screened at the water table, while during Phase 2 dual-phase extraction was performed at the same well. The application of 27 kPa vacuum resulted in an increase in NAPL recovery from negligible (Phase 1) to approximately 6.6 l/d (Phase 2), with a concurrent increase in water recovery from approximately 190 to 760 l/d. Neutron moisture probe observations revealed that vadose-zone liquids underwent redistribution toward the extraction well in response to the onset of Phase 2, also in accordance with the conceptual model. An understanding of soil physical relationships is crucial to the successful application of these and other *in situ* soil remediation technologies.

KEY WORDS: vadose zone, multiphase flow, *in situ* remediation, dual-phase extraction, bioslurping, pilot test.

I. INTRODUCTION

During the remediation of hydrocarbon-contaminated sites, the usual initial step if free product is present is its recovery by direct pumping from extraction wells or

trenches. Typically, however, such methods cease to be effective long before the nonaqueous-phase liquid (NAPL) has been completely removed because they cannot overcome the capillary forces that retain the remaining NAPL within soil or fractured rock pores. Vacuum-enhanced free-product recovery may be used to help overcome these capillary forces. A conceptual model is presented that helps to explain why, and under what conditions, vacuum-enhanced recovery can be effective. The utility of this approach is also illustrated by the results of a field test.

A method now in widespread use for the *in situ* remediation of hydrocarbon-contaminated sites is soil vapor extraction (SVE). SVE focuses on inducing volatilization of NAPL and vapor-phase transport of volatile organic compounds (VOCs) from the subsurface to the surface for subsequent treatment (U.S. EPA, 1991). Increasingly, the concurrent aeration of the subsurface that occurs during SVE is being used to enhance *in situ* bioremediation of nonvolatile as well as volatile compounds in a process known as bioventing (Dupont *et al.*, 1991). For the most part, the attention of SVE and bioventing practitioners has been on vapor phase transport. Theoretical treatments of SVE frequently adopt the assumptions that variable water saturations in the unsaturated zone can be ignored (Johnson *et al.*, 1990; Marley *et al.*, 1990) or that liquid phases are immobile or unaffected by variations in gas-phase pressure (Baehr and Hult, 1988; Gierke *et al.*, 1992; Shan *et al.*, 1992; Sleep and Sykes, 1989). The effects of gas phase-pressure on the equilibrium saturation of porous media, however, have long been recognized (Cassel and Klute, 1986; Vachaud *et al.*, 1973). Such effects are observed especially in bounded systems within which the applied pneumatic potential cannot be converted to kinetic energy (e.g., air flow) as it is in unbounded systems. A common laboratory example is the use of a vacuum chamber to saturate soil samples that are immersed within. The effects of gas-phase pressure on equilibrium saturation are here recognized to extend to open systems in which an applied pneumatic potential induces both pneumatic and hydraulic gradients.

SVE and bioventing are rarely methods of choice when significant volumes of free product remain in the subsurface. Using an approach somewhat related to SVE, however, Blake and Gates (1986) and Hayes *et al.* (1989) describe the application of vacuum-enhanced free-product recovery methods at several remediation sites. Such methods involve the application of a vacuum to a single well or a multiwell system while performing liquid recovery. They attribute the success of these methods to the increased effective drawdown created by vacuum-assisted pumping. In a related application, vacuum drainage methods employing reductions in air-phase pressure have been reported by construction dewatering engineers for enhancing the removal of water retained by capillary forces in medium- to fine-textured soils.

II. CONCEPTUAL MODEL

When light nonaqueous phase liquid (LNAPL) is present in soils that have positive entry pressures (e.g., Brooks-Corey porous media), (Corey, 1986) LNAPL may not

be observed in monitoring wells (Farr *et al.*, 1990). A reduction in gage pressure in such media, however, will tend to release LNAPL, along with water, into the well, provided the air pressure in the well is less than the nonwetting entry pressure (i.e., $P_{sub} < P_b$). Here, P_{sub} indicates a pressure less than atmospheric pressure induced within a well-screened through portions of both the vadose and saturated zones, and P_b is the nonwetting entry or displacement pressure of the medium. Figure 1 illustrates the analogous case of application of an air pressure less than atmospheric to a wetted soil sample situated on a porous plate. If $P_{sub} < P_b$, a fraction, f_a , of the porosity of the soil will desorb, provided that the larger pores within the medium are interconnected. In effect, this application of vacuum causes a translation of the abscissa of the pressure saturation curve upward by a magnitude

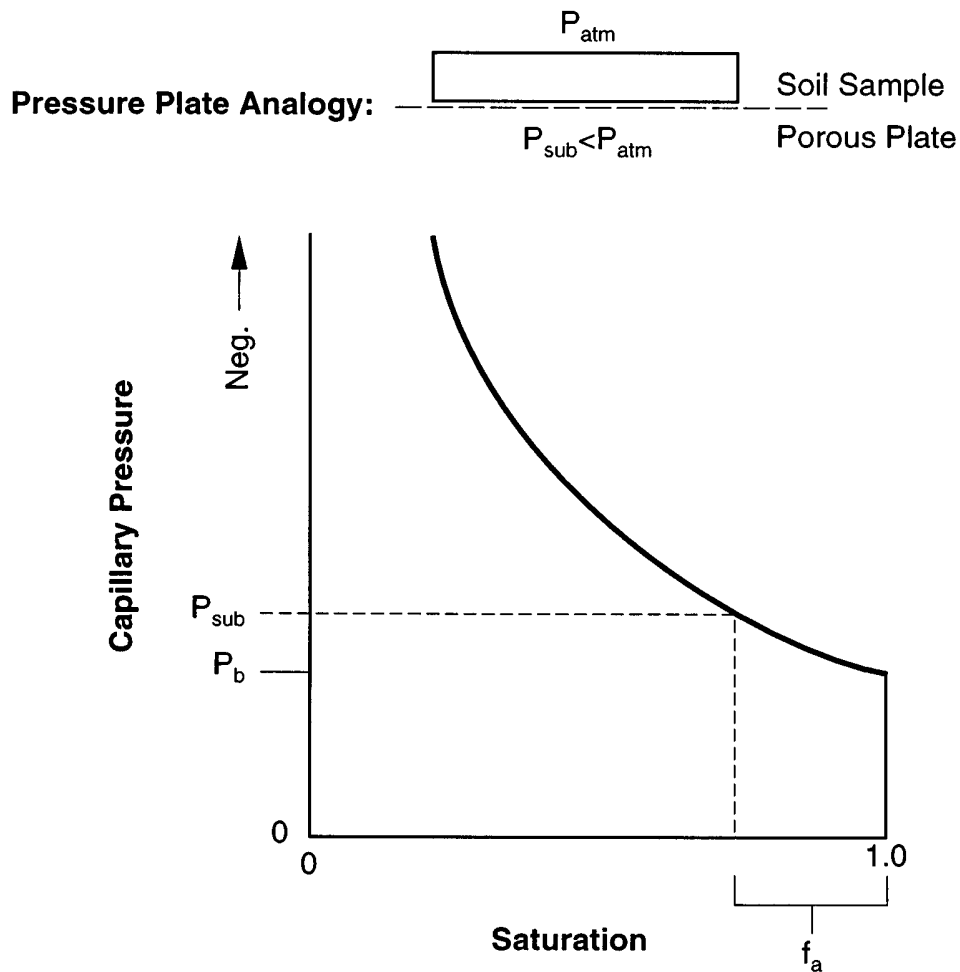
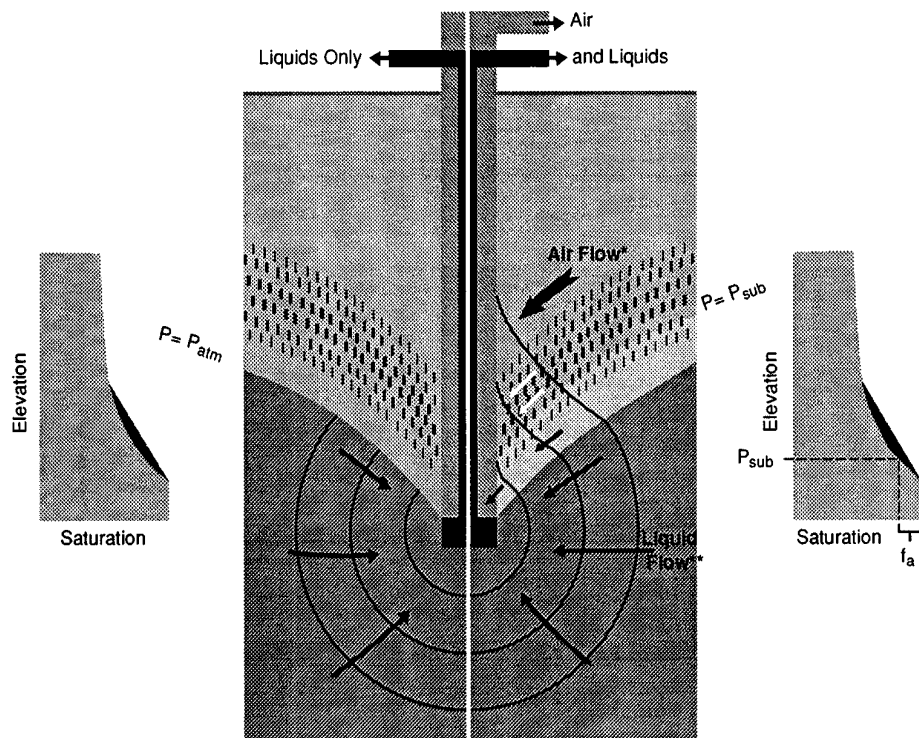


FIGURE 1. Effect on soil water of a reduction in soil air pressure.

equal to P_{sub} , with the potential energy per unit volume (i.e., pressure) of all the water in the system being commensurately increased by the same magnitude. Similarly, in media having zero entry pressures, application of a subatmospheric pressure to the well will allow water and oil to be released into the well that previously were prevented from doing so by capillary forces.

This conceptualization was examined by the performance of an *in situ* pilot test in which both air and liquids were withdrawn from the same well over a 3-week period. We sought a qualitative indication that liquid recovery is enhanced during such a test, and insight into the nature of the phenomenon that will assist in the predictive modeling of such effects. To make the effects of the test easier to discern, the simultaneous withdrawal of both air and liquids from the subsurface was conducted so as to create a dynamic equilibrium (quasi-steady state condition).

The anticipated effects of the pilot test are presented schematically in Figure 2. Specifically, the two halves of Figure 2 compare the effects of extraction of liquids



* Air flows in response to pneumatic gradients induced by application of vacuum ($P=P_{sub}$) in well.

** Liquid flows in response to hydraulic gradients induced by drawdown of piezometric surface and enhanced by application of vacuum ($P=P_{sub}$) in well.

FIGURE 2. Effect of vacuum extraction on liquids recovery.

only vs. extraction of liquids plus vapor. The left-hand half of the central figure depicts a cross-sectional view through a subsurface formation penetrated by an extraction well, as well as the distributions of water and LNAPL that prevail after the pumping of liquids (by means of a double-diaphragm pump with a fixed intake elevation) has been conducted long enough to establish a steady-state cone of depression. As no vapor is extracted, the air pressure in the well is equal to atmospheric pressure. The phreatic surface (i.e., the water table), having a pressure equal to atmospheric pressure, is indicated by the curve marked $P=P_{\text{atm}}$. Below the water table, equipotential lines and perpendicular flow lines indicate that water is being extracted as fast as it is able to flow into the pumping well. The smaller plot to the left side of the schematic, however, presents the equilibrium distribution of vadose water and LNAPL (dark shading) that exists in a cylindrical control volume adjacent to the well, at and above the elevation of the water table. LNAPL residing within a fraction of the pores of the capillary fringe, indicated by vertical stipling on the left side of the central figure of Figure 2, cannot flow into the extraction well because $P_b < P_{\text{atm}}$. Vadose water cannot flow into the extraction well for the same reason, under these equilibrium conditions. Note that the use of stipling is not meant to imply that the NAPL resides solely in noninterconnected pores.

The right-hand half of the central figure of Figure 2 shows what is expected to occur following steady application of P_{sub} and withdrawal of air from the extraction well, while the recovery of liquids is continued as fast as they are able to flow into the pumping well. The reduction in gage pressure within the well that accompanies vapor extraction is widely recognized to induce a pressure gradient within the gaseous phase that causes vapor to flow from zones of higher air pressure toward the well (Johnson *et al.*, 1990). Less widely recognized is that the reduction in gage pressure within the well also causes an upward and inward translation of the potentiometric surface that is in equilibrium with the air pressure within the well from the former position to the curve marked $P=P_{\text{sub}}$. As a result, water and LNAPL residing between the former water table and the new curve marked $P=P_{\text{sub}}$ (i.e., within the light-colored area) can now enter the well, inducing liquid flow parallel to the water table. The plot to the right side of the schematic indicates how a portion of the vadose water and LNAPL will potentially be recovered that was hitherto nonrecoverable.

We may term this translation of the potentiometric surface “inwelling” (Baker and Wiseman, 1992), in contrast to the “upwelling” (Pedersen and Curtis, 1991) that occurs when a vacuum is exerted in an SVE well screened above the water table. Along with the inwelling of the surface at which $P=P_{\text{atm}}$ shown in Figure 2, a family of concentric surfaces of various pressures both greater than and less than atmospheric pressure would all concomitantly translate toward the well, thereby increasing the hydraulic gradient in both the saturated and unsaturated zones that serves as the driving force for liquid flow.

If a great enough vacuum could be gradually applied to the well without inducing shortcircuiting, theoretically all of the NAPL residing in interconnected pores within the zone of influence of the extraction well (as well as a good deal of vadose water) could be recovered in this fashion. Even if some fraction of the NAPL were left behind, as from “snapping off” of formerly connected NAPL ganglia, the remaining immobile (“residual”) NAPL would then be more amenable to being remediated by other *in situ* techniques, such as SVE or bioventing, because the NAPL-air interfacial surface would be larger.

In actuality, the gaseous-phase pressure exerted on the soil surrounding the well screen during vacuum-enhanced liquids recovery will not be as low as P_{sub} , because in an unbounded system, unlike the case of Figure 1, the gaseous-phase pressure head diminishes with distance from the well screen. This head loss results from the geometry of the system (i.e., because the vacuum’s intensity is dissipated radially with distance from the well) and from the conversion of energy. As the kinetic energy of the gaseous phase increases with vacuum-induced air flow, the potential energy per unit weight (i.e., pressure head) of the system is reduced commensurately, in accordance with Bernoulli’s law and the conservation of energy.

III. METHODS

A. Background

A pilot test was performed at the ThermalKEM facility, Rock Hill, SC. A known area of concern (AOC) at the facility contains fuel oil (diesel) formerly released into the subsurface through underground piping. The AOC is located between a pump house EW-1 and the diesel fuel pump station (Figure 3). Analyses of the lateral and vertical extent of the LNAPL were conducted to determine product volumes, with 14,000 and 184,000 gal of free product being estimated to be present in this area.

The typical stratigraphy, from the surface downward, for the AOC consists of 1 to 3 ft of gravelly fill, 10 to 15 ft of silty clay, and 10 to 15 ft of saprolite, underlain by fractured gabbro bedrock. The saprolite is a very compact silty sand located at the weathered uppermost zone of the gabbro rock formation. The top of the product layer observed in the monitoring wells is located at 13 to 15 ft beneath the ground surface, and the product that accumulates in monitoring wells is several feet thick in some areas.

B. Equipment Installation

1. Wells, Piezometers, and Soil Samples

Figure 3 is a site plan illustrating the location of monitoring installations and pumping wells. Figure 4 is a schematic cross-section illustrating the relative

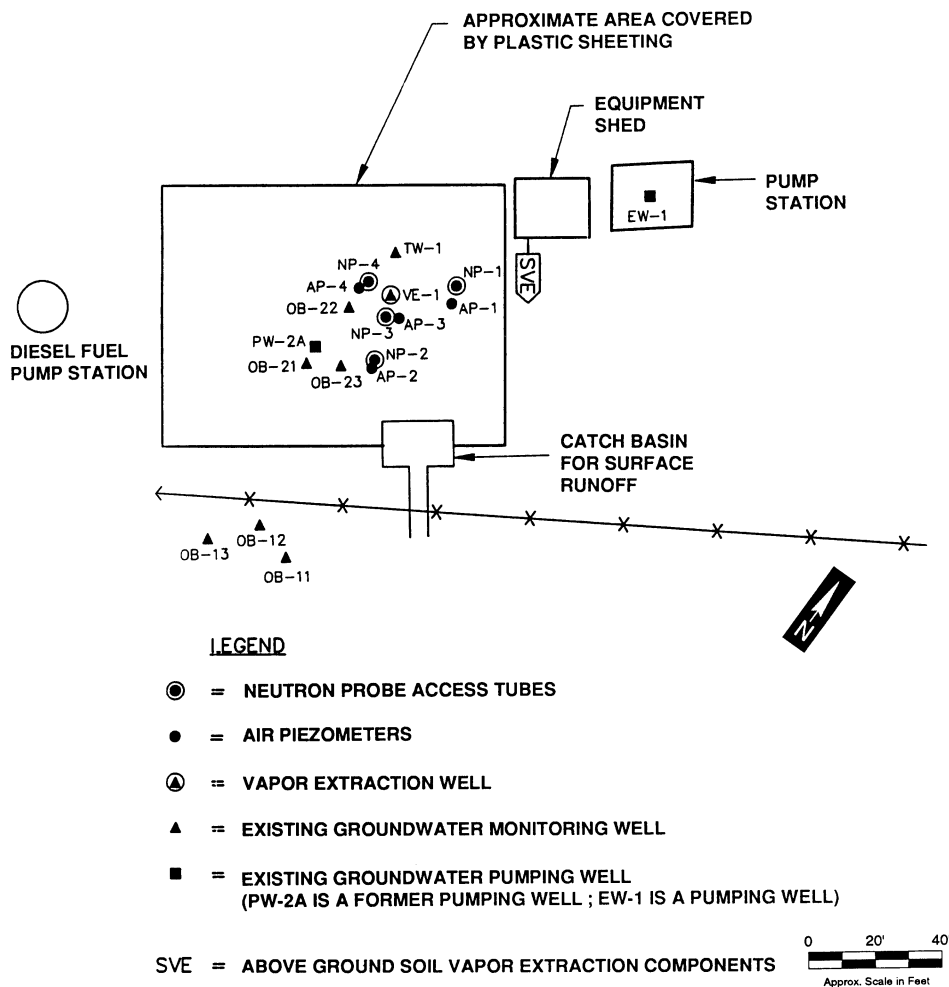


FIGURE 3. Site layout plan.

elevations of the various subsurface components of the vacuum-enhanced recovery system pilot test.

A vapor/liquid extraction well (VE-1) was installed consisting of 4-in. Schedule 40 PVC pipe screened from approximately 3 to 28 ft below ground surface (bgs). Already existing at the site of the field test were a number of monitoring wells and a former pumping well (Figure 3). An array of four nests of air piezometers (3/8 in. I.D., Schedule 80 PVC), two air piezometers per nest, were installed radially outward from VE-1 at angular intervals of approximately 120°. The piezometers, installed using hollow-stem augers, consisted of open-ended pipe ending midway within a 1 ft thick sand pack located at depths

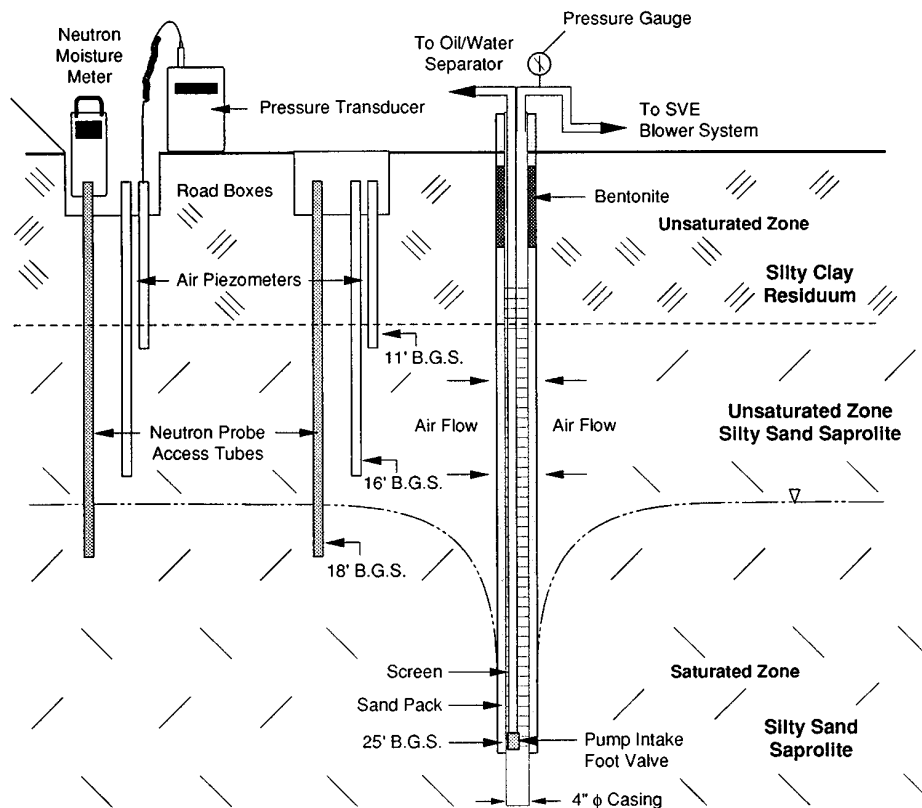


FIGURE 4. Schematic of subsurface air and groundwater withdrawal and monitoring.

of 11 ft and 16 ft bgs. All air piezometer (AP) tubes were located 2 to 3 ft from a neutron probe access tube. The neutron probe (NP) access tubes consisted of 1.5-in. Schedule 40 PVC pipe that was pushed into air rotary drilled boreholes. NP access tubes NP-1, NP-2, NP-3, and NP-4 were placed to depths of 18 ft, 18 ft-2 in., 20 ft, and 17 ft-2 in. bgs, respectively. A minimum of 1 ft of bentonite was placed around the top of each neutron access tube and AP to prevent shortcircuiting of air during vapor extraction.

Soil samples for physical parameters were collected during the installation of the APs. A lined split spoon was retrieved from two of the AP locations (AP-3 and AP-4) from depths of 15 to 17 and 10 to 12 ft bgs. Undisturbed soil samples for physical parameters were obtained by cutting the bottom 6 in. of the lined split spoon sample.

2. Total Fluids Recovery System

A total fluids recovery system was installed to extract both LNAPL and groundwater in a single conduit and separate the two phases in an aboveground oil/water separator. During system operation, groundwater was extracted from the well with a double-diaphragm pump located adjacent to the well. These pumps can run dry without being damaged. A foot valve located near the bottom of the well was installed at the end of the intake line. The total fluids stream was pumped to the oil/water separator.

3. Pilot Soil Vapor Extraction System

An ENSR-supplied, trailer-mounted mobile SVE system was transported to the site, and the required piping and wiring were installed to allow soil vapor to be extracted from VE-1. The vacuum blower was a Sutorbilt Model GHVF-BHC, 15-HP with an operating vacuum of 8 in. Hg. A well head was constructed to accommodate simultaneous vapor and liquid recovery from the well and to allow both vacuum levels and air-flow rate to be measured at the well.

A temporary surface seal was installed in the vicinity of VE-1 to prevent shortcircuiting by covering a 100 × 75-ft area with 20-mil-thick polyethylene sheets. The sheets were cut and taped around the monitoring and extraction wells. Clean fill material was placed around the perimeter of the liner to hold the seal in place.

C. Process Monitoring and Operation

The pilot test was designed to evaluate and compare approaches to the recovery of fuel oil from the water table, as well as supply information necessary to design and implement a full-scale remedial system. The pilot test was conducted in separate phases. Phase 1 involved pumping liquid only from well VE-1 for 4 d to establish a fuel oil recovery rate; Phase 2 combined soil vapor extraction with pumping of liquid for 3 weeks to assess the enhancement of liquid recovery during vapor extraction. The test also provided information necessary to characterize the rate of vapor phase VOC removal, the extent of vacuum influence, soil permeability, and the initial effect of SVE on biological activity (potential for bioventing).

During the 3-week period of phase 2, the SVE system was inadvertently shut down on two occasions, day 2 and days 9 and 10 of the test, because of power loss to the system. These events presumably allowed resaturation of the soil within the cone of depression surrounding extraction well VE-1.

The SVE blower system (15 hp) was able to exert a vacuum at well VE-1 of between 7.0 and 8.0 in. Hg during the test. The average air-flow rate from the well

was 3.5 standard cubic feet per minute (SCFM). The measured air-flow rates are relatively low for the amount of vacuum applied and are related to the low permeability of the subsurface. To avoid overheating of the blower at a selected blower speed, it must be operated within a predetermined vacuum and air-flow range. Due to the low air flow from VE-1, the system required a large amount of fresh dilution air to operate normally. The dilution valve was set open during blower start-up and was to be closed in increments so as to apply higher vacuum levels during the test. However, because of the dense soils, the blower fresh air valve could not be closed and the vacuum levels could not be altered.

Pressure readings in selected monitoring wells (OB-13, TW-1) and APs (AP-1 through AP-4, shallow and deep) were recorded with a pressure transducer (Tensimeter™) on each day (except weekends 10/3 to 10/4 and 10/10 to 10/11). Air velocity and temperature were measured at the well and at the blower as actual cubic feet per minute (ACFM) readings and were converted to SCFM.

Two totalizing flow meters were monitored daily during phases 1 and 2 to assess the volume of liquid and fuel oil recovered.

IV. RESULTS AND DISCUSSION

A. Physical Soil Data Results and Discussion

Table 1 summarizes the data obtained from physical analyses of core samples obtained during installation of the two AP nests located 5 ft to the south and west-northwest of extraction well VE-1. Samples AP-3S and 4S were obtained from a depth of 11 ft bgs, while samples AP-3D and AP-4D were obtained from a depth of 16 ft bgs.

The two cores collected were split for a total of four samples, which were analyzed for determination of saturated hydraulic conductivity, grain-size distribution, moisture content, bulk density, moisture retention curves, and organic carbon content. Bulk density, the moisture retention curve, and saturated hydraulic conductivity can be used to estimate relative soil permeability, which is a critical design parameter of the scaled-up SVE system. Retention curves and organic carbon content provide an indication of the tenacity with which liquids and VOCs will be held in the soil matrix.

The moisture retention analysis (Klute, 1986) involves the stepwise application of a pressure differential to an initially saturated soil sample, with the equilibrium moisture content measured at each step. The first step involves application of the lowest (e.g., 15.6 mbar, equivalent to 6.26 in. of H₂O) pressure step to the sample, which induces drainage of water from the largest pores of the sample until equilibrium is approached at that pressure, at which time the sample is weighed to determine the volume of water desorbed from those pores. Then the next higher pressure is applied, inducing drainage from the next smaller class of pores, and

TABLE 1
Summary of Physical Soil Analysis Data

Parameter	Sample #			
	AP-3D-HC	AP-4D-HC	AP-3S-HC	AP-4S-HC
Saturated hydraulic conductivity (cm/s)	2.3×10^{-4}	4.1×10^{-4}	3.2×10^{-4}	8.5×10^{-5}
Initial moisture content				
Gravimetric (% g/g)	10.53	14.39	16.67	30.30
Volumetric (% cc/cc)	19.87	24.41	26.83	44.27
Dry bulk density (g/cc)	1.89	1.70	1.61	1.46
Calculated porosity (%)	28.83	35.99	39.27	44.87
Particle size characteristics				
d_{10}	0.03	0.0087	0.0095	0.004
d_{50}	0.32	0.16	0.18	0.08
d_{60}	0.46	0.23	0.28	0.13
C_u	15	26	29	33
C_c	0.02	1.74	1.84	0.62
Gravimetric % (g/g)	9.85	15.85	16.84	28.34
Total organic carbon (g/kg)	1.7	2.2	2.0	2.9
Soil moisture retention data	Moisture content (% cm^3/cm^3)			
	AP-3D-HC	AP-4D-HC	AP-3S-HC	AP-4S-HC
Suction (cm water)				
0	32.27	38.78	40.07	47.17
32	31.60	37.39 ^a	38.80	47.14 ^b
78	27.32	33.24	34.19	46.21
	AP-3D-PP	AP-4D-PP	AP-3S-PP	AP-4S-PP
0	31.29	40.47	40.29	47.01
255	21.19	26.77	27.82	41.90
1020	17.77	20.10	21.11	34.24
3059	15.56	16.58	18.08	27.39
5297	13.67	14.15	15.69	26.08
32073 ^f	9.30	8.48 ^c	9.94 ^d	11.21 ^e

Note: HC, hanging column test sample; PP, pressure plate test sample.

^a Moisture content at – 33 cm water.

^b Moisture content at – 35 cm water.

^c Moisture content at – 19621 cm water (thermocouple psychrometer data).

^d Moisture content at – 11870 cm water (thermocouple psychrometer data).

^e Moisture content at – 20906 cm water (thermocouple psychrometer data).

^f Thermocouple psychrometer data.

reequilibration is allowed to occur, followed by reweighing. The process thus proceeds in a stepwise fashion, until the sample is virtually dry.

To save time, each sample submitted to the laboratory consisted of two adjacent cores, not for the purpose of providing duplicate analyses, but to enable simulta-

neous evaluation of the low and high ends of the desired pressure range. The low-pressure end of the pressure range is obtained using a hanging water column, while a pressure plate extractor is used to obtain the high-pressure end, with the highest (e.g., 15 bar) pressure point being obtained using a thermocouple psychrometer (Rawlins and Campbell, 1986). The resulting data are plotted as matric suction vs. moisture content (or pressure vs. saturation) and comprise one of the fundamental constitutive properties of the porous media.

Generally speaking, samples AP-3D, AP-4D, and AP-3S were similar with respect to permeability, grain-size distribution, pore-size distribution, bulk density, and moisture content, while AP-4S was finer in texture, lower in permeability, more fine-porous, and had a higher water content as received from the field. Comparison of percent moisture data with the soil moisture retention curves indicates that the soils represented by the three similar cores were 50 to 60% saturated by liquid at the beginning of the pilot test, while the soil represented by AP-4S was nearly saturated at that time. The four samples reflect a spatial variability and heterogeneity that is to be expected based on the stratigraphy observed during soil boring. It appears that none of the cores intersected a major saprolite fracture zone.

The soil cores are compact, silty sands (USCS classification), with a predominance of fine pores that would be expected to restrict the movement of fluids.

B. Evaluation of the Volume of Recoverable Fuel Oil

The determination of pressure-saturation curves (also referred to as soil moisture retention curves) for the four undisturbed cores mentioned in the previous section enabled estimation of the volume of recoverable fuel oil at the AOC.

Previously, site-specific parameters for free-product estimation models (Farr *et al.*, 1990; Lenhard and Parker, 1990) were unavailable, and volume estimates had been based on a physical interpretation of product and groundwater baildown tests. Once site-specific parameters became available, the model of Farr *et al.* (1990) was employed to reestimate free-product volumes at the AOC. The model assumes static equilibrium, uses measured interfacial tension and density of the fluid (fuel oil), and measured pressure-saturation relationships for the porous medium (saprolite). Only continuous NAPL volume is considered by this method; residual product is not accounted for.

The results indicated that the NAPL formation thickness ranged from 0.03 to 5.1% of the NAPL thickness observed in a given well, depending on the product thickness observed in the well and which soil parameters obtained from the cores were used as input. This very low percentage of true relative to apparent free-product thickness is not surprising, given the compact and fine-porous nature of the saprolite core samples. Although it is commonplace to conceive of the oil as floating on the water table, in a fine-porous medium such as this, most of the finer

pores in the zone above the capillary fringe tend to retain water, not oil. Therefore, only a fraction of the pores in and above the capillary fringe zone contain oil, according to the Farr *et al.* (1990) model, a finding of great relevance to the free-product recovery test results.

Based on upper and lower estimates of the areal extent of the affected area, the model's estimate of recoverable free product in the formation ranges from 14,000 to 184,000 gal. A larger number of core samples and a better areal delineation of the plume would be required to narrow this range.

C. Results of Phase 1 — Fuel Oil Recovery

The field pilot test was undertaken with a primary objective of evaluating alternatives for removing fuel oil from the subsurface. It was necessary to establish an initial product recovery rate from VE-1 as a standard by which to measure the other work phases.

In the 4 d of the phase 1 operation, oil accumulated as a floating layer on the water in the oil-water separator but was insufficient in volume to allow separation, and was estimated to represent less than 1 gal/d of fuel oil recovery.

D. Results of Phase 2 — Application of Vacuum

1. Measured Effects of Vacuum Vs. Distance

Figures 5 and 6 present the AP pressure readings observed during the 21-d SVE pilot study, along with concurrent daily precipitation data. Specifically, Figure 5 illustrates readings obtained from APs located 5 ft laterally from VE-1, at the same locations and depths from which the aforementioned soil samples for physical and chemical analyses were derived. Figure 6 shows comparable readings obtained from APs located 15 ft laterally from VE-1. On these graphs, positive pressures indicate air at pressures greater than atmospheric pressure, while negative pressures indicate air at pressures less than atmospheric pressure (i.e., subject to vacuum).

The greatest overall influence of the vacuum was detected at AP-3S (S indicates shallow, 11 ft bgs, whereas D indicates deep, 16 ft bgs). This was also the only AP 5 ft from the extraction well that showed a continuous vacuum throughout the study. The fact that the other three of the nearest APs detected vacuum for only portions of the study reflects the heterogeneous nature of the saprolite formation. Because the permeability of the saprolite to air tends to be controlled largely by whether or not the fractures are saturated with liquid, it appears that periods occurred during which such fractures near a given piezometer (e.g., AP-4S and AP-4D) became unsaturated and subject to air flow, as from days 2 to 6, followed

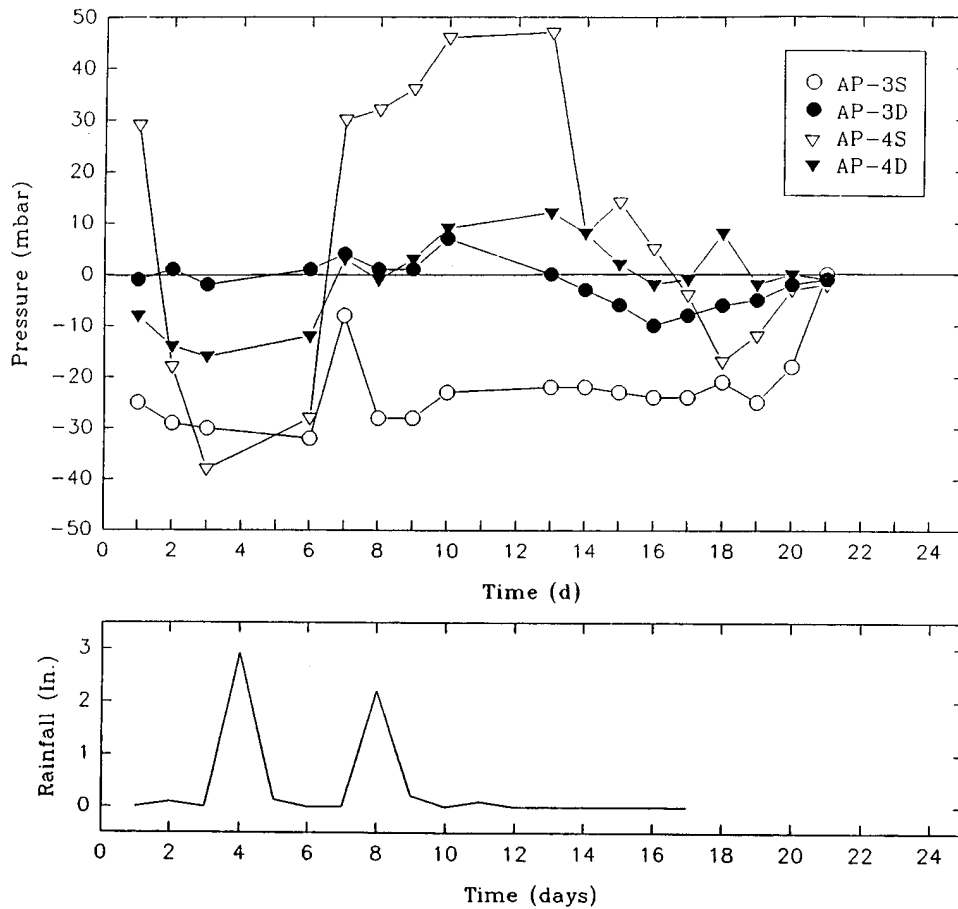


FIGURE 5. Air piezometer readings 5 ft laterally from VE-1, with concurrent precipitation data.

by a period of resaturation and occlusion of air flow, as from days 7 to 13. The most likely explanation for these changes is the effect of two large rainstorms that took place on day 4 (2.94 in. of rain) and day 9 (2.21 in.) (Figure 5). After the storms, the influence of the vacuum well generally declined. Only after day 13 did the soil begin to dry out slightly — enough to show, for a few days, a general increase in vacuum readings.

Of those APs located 15 ft from VE-1 (Figure 6), only the two shallower units (AP-1S and AP-2S) showed a nearly continuous vacuum. The influence of VE-1 was reduced relative to what was experienced at the closer AP-3S. Only in the southerly direction does the combination of AP vacuum readings from 5 and 15 ft from VE-1 potentially lend itself to the modeling of *in situ* permeabilities. The suspected anisotropy in air permeabilities, however, limits the applicability of

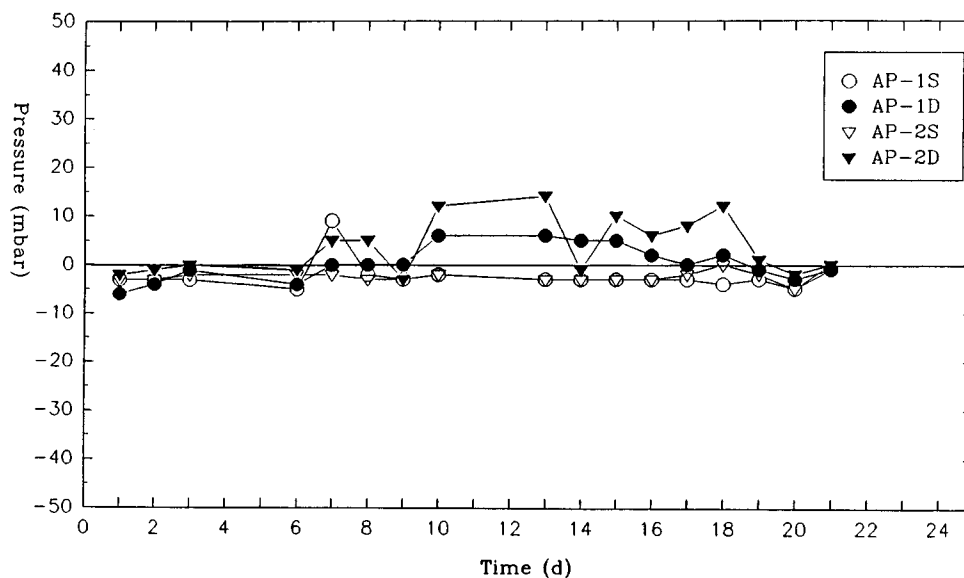


FIGURE 6. Air piezometer readings 15 ft laterally from VE-1.

available models to this site. Therefore, if SVE is utilized in the future to remediate residual soil contamination, well spacing would need to be determined empirically based on the observed effects of vacuum with distance, rather than on a specific modeling effort.

Overall, the influence of the vacuum well appears to have been uneven over space and time and subject to rainfall events. The influence of the vacuum extended at least 15 ft in two out of the three directions monitored, and was generally greater at shallower depths in the saprolite.

E. Soil Saturation and Liquids Recovery as Influenced by Vacuum Extraction

Two to four ft laterally from each AP nest, a neutron access tube was installed to enable the degree of saturation of the formation to be repeatedly monitored. Neutron depth moisture gauges precisely detect the presence of hydrogen-rich materials (water and hydrocarbons) but cannot discriminate between them (Kramer *et al.*, 1992).

Figure 7 presents the volume fraction of the soil (at depths of 11 and 16 ft bgs, corresponding to the depths of the APs) that was occupied by water or NAPL, as determined by neutron thermalization. The radius of influence of neutron moisture probes varies with hydrogen density. For the nearly saturated soils for which data

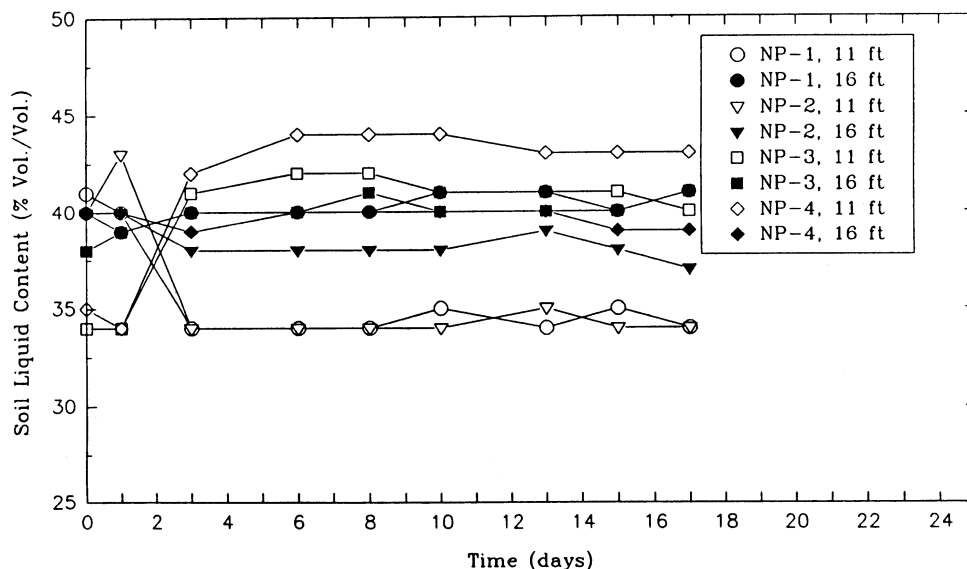


FIGURE 7. Soil liquid results.

are presented in Figure 7, the spherical volumes that were monitored around the probe probably ranged from 6 to 12 in. in radius. Therefore, they were larger in scale than the soil core samples and would have had a larger likelihood of intersecting minor, if not major, saprolite fractures. Only one or two laterally continuous minor fractures would have needed to become desaturated (air filled) within such a volume to have accounted for a measurable air flow. (Note that when a porous medium undergoes desaturation, the largest pores or fractures are the first to drain.)

Figure 7 indicates that after day 3, the NP readings became quite steady, with the soil remaining generally quite saturated by water and/or NAPL. Between days 1 and 3, however, the two shallow locations 5 ft to either side of the extraction well became significantly more saturated, while the two shallow locations 15 ft to either side of the extraction well became concomitantly less saturated. This observation is generally borne out, within the saprolite, at the other depths monitored that are not reported in Figure 7. This redistribution of vadose-zone liquid toward the extraction well is evidence of the inwelling of vadose-zone liquid predicted by the conceptual model, and was anticipated by McWhorter (1990). In the present pilot study, this flow toward the extraction well appeared to approach a steady state.

As indicated in Figure 8, the rates of both water and fuel recovery were greater after application of vacuum, compared with the prevacuum recovery rates, again in accord with theory. Although the recovery of diesel fuel was rather paltry (about 55 gal total), virtually none had been recovered prior to the application of vacuum. Meanwhile, about 200 gpd of water was recovered during SVE, compared with about

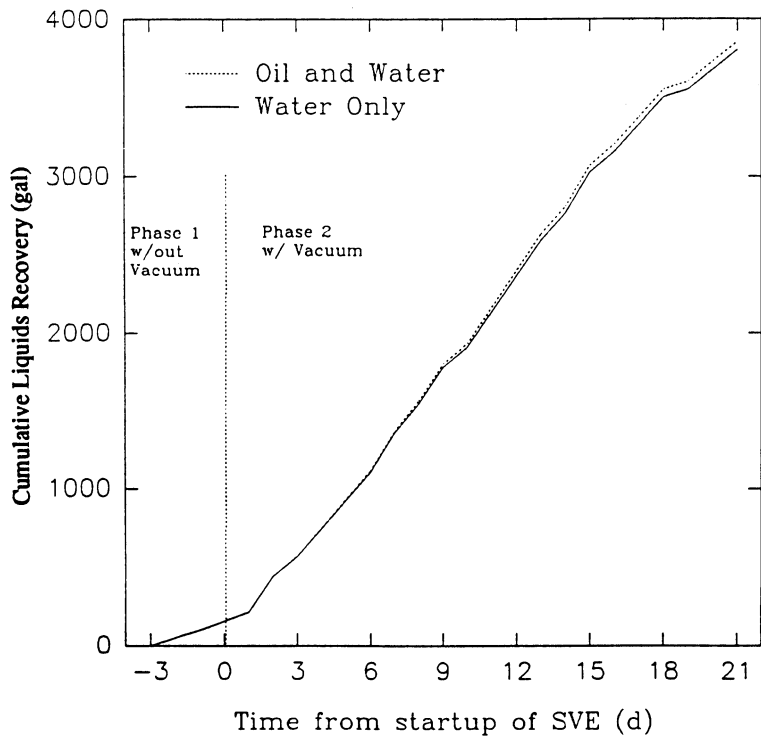


FIGURE 8. Liquids recovery.

50 gpd during conventional pumping only. The disproportionately larger volume of water than NAPL recovered is consistent with the distribution predicted by the model of Farr *et al.* (1990), as described in Section IV.B. The amount of fuel oil recovered after the application of the vacuum averaged 1.75 gpd. An increase in oil recovery is obviously desirable; an increase in groundwater recovery, however, places an additional load on water treatment facilities and is therefore less desirable.

The pilot blower employed applied a vacuum of about 7 to 8 in. Hg to the extraction well. Theoretically, application of an even higher vacuum (e.g., 20 in. Hg) during free-product recovery in this formation should release a proportionately higher fraction of vadose water and NAPL now retained in smaller pores by capillary forces. Drawbacks to such an approach are that high vacuums can promote shortcircuiting of flow and more pronounced upwelling and inwelling of the water table and capillary fringe toward the extraction well.

F. Water and Product Gauging Results

Water level and product elevations were measured in select monitoring wells daily during the 3-week test. These data were collected to provide an indication of the

effects groundwater pumping had on water/product elevation and to determine a pumping radius of influence.

In general, the wells within 20 ft of VE-1 were influenced by VE-1 pumping, while wells beyond 20 ft of VE-1 were not. This finding is consistent with the expected results, given that the entire fuel oil area was continually influenced by groundwater pumping of the underlying bedrock aquifer at well EW-1.

G. Effects of Secondary Permeabilities on Liquid/Product Recovery

Liquid recovery data are depicted in Figure 8 and discussed in the previous sections. Certain data collected during this test, including air and liquid flow rates into extraction well VE-1, are indicative of heterogeneous conditions in the subsurface. The measured effects of vacuum at APs located at different angular positions (Figures 5 and 6) show a much greater effect at AP-3 (fairly consistent -30 mbar pressure) than at AP-4 (general positive pressures). The effects of heterogeneity are also clearly evident in recovery data subsequently obtained from other onsite wells. These data indicate that certain wells are located in more productive zones and therefore yield higher average liquid and product recovery rates.

V. CONCLUSIONS

As demonstrated in the field test and as predicted by theory, SVE should be regarded as potentially capable of inducing the flow of liquids through the vadose zone into an extraction well, especially in medium- and fine-textured soils in which the vapor and liquid air pressures can be reduced by the application of a vacuum. This may have both positive and negative side effects: It may increase the recovery of free product (desirable), but may also increase the volume of water containing dissolved contaminants that may require treatment prior to discharge. For both reasons, more attention to these phenomena is needed, so that properly designed and effective remediation systems can result.

The effectiveness of vacuum to enhance fuel oil recovery and reduce soil gas at the test site may be summarized as follows:

1. The application of vacuum appeared to result in an increase in fuel oil recovery at VE-1 from negligible to approximately 1.75 gpd, along with an increase in water recovery of from approximately 50 to 200 gpd, in accordance with the conceptual model.
2. Application of even higher vacuums would be expected to produce proportionately higher yields of both free product and water, if short-circuiting could be avoided.
3. The effectiveness of SVE to reduce soil gas concentrations was demonstrated during the pilot study, but would tend to be limited by the uneven

influence of the applied vacuum within the saprolite formation, and is not indicative of extensive vapor-phase product recovery.

4. The effectiveness of the vacuum on enhancement of both fuel oil recovery and soil vapor extraction at this site is influenced strongly by the fracture- and pore-size distribution within the saprolite, which controls its permeability and liquid retention properties.

ACKNOWLEDGMENT

The authors are grateful to Jeff Munic for his contributions to the design and construction of the pilot test.

REFERENCES

- Baehr, A. L. and Hult, M. F. 1988. Determination of the air-phase permeability tensor of an unsaturated zone at the Bemidji, Minnesota, research site. **In:** U.S. Geological Survey Toxic Substances Hydrology Program — Proceedings of the Technical Meeting, p. 55. (Mallard, G. E. and Ragone, S. E., Eds.) Phoenix, AZ, September 26 to 30.
- Baker, R. S. and Wiseman, J. T. 1992. Importance of vadose zone monitoring during soil vapor extraction pilot studies. **In:** Proc. Int. Symp. In Situ Treatment of Contaminated Soil and Water, Air & Waste Management Assoc., p. 26. Cincinnati, OH, February 3 to 6.
- Blake, S. B. and Gates, M. M. 1986. Vacuum enhanced hydrocarbon recovery: a case study. **In:** Proc. Petroleum Hydrocarbons and Organic Chemistry in Ground Water: Prevention, Detection and Restoration Conf. p. 709. November.
- Cassel, D. K. and Klute, A. 1986. Water potential: tensiometry. **In:** *Methods of Soil Analysis, Part I. Physical and Mineralogical Methods*, p. 563. (Klute, A., Ed.) Agronomy Monogr. No. 9, 2nd ed. Madison, WI, American Society of Agronomy-Soil Science Society of America.
- Corey, A. T. 1986. Mechanics of Immiscible Fluids in Porous Media. Littleton, CO, Water Resources Publications.
- Dupont, R. R., Doucette W. J., and Hinchee, R. E. 1991. Assessment of *in situ* bioremediation potential and the application of bioventing at a fuel-contaminated site. **In:** *In Situ Bioreclamation*, p. 262. (Hinchee, R. E. and Olfenbittel, R. F., Eds.) Stoneham, MA, Butterworth-Heinemann.
- Farr, A. M., Houghtalen R. J., and McWhorter, D. B. 1990. Volume estimation of light nonaqueous phase liquids in porous media. *Ground Water*. **28(1)**:48.
- Gierke, J. S., Hutzler N. J., and McKenzie, D. B. 1992. Vapor transport in unsaturated soil columns: implications for vapor extraction. *Water Resour. Res.* **28(2)**:323.
- Hayes, D., Henry, E. C., and Testa, S. M. 1989. A practical approach to shallow hydrocarbon recovery. *Ground Water Monit. Rev.* Winter, 180.
- Johnson, P. C., Kemblowski, M. W., and Colthart, J. D. 1990. Quantitative analysis for the cleanup of hydrocarbon-contaminated soils by in-situ soil venting. *Ground Water*. **28(3)**:413.
- Klute, A., 1986. Water retention: laboratory methods. **In:** *Methods of Soil Analysis, Part I. Physical and Mineralogical Methods*, p. 635 (Klute, A. Ed.) Agronomy Monogr. No. 9. 2nd ed. Madison, WI, American Society of Agronomy-Soil Science Society America.
- Kramer, J. H., Cullen, S. J., and Everett, L. G. 1992. Vadose zone monitoring with the neutron moisture probe. *Ground Water Monit. Rev.* Summer, 177.

- Lenhard, R. J. and Parker, J. C. 1990. Estimation of free hydrocarbon volume from fluid levels in monitoring wells. *Ground Water*. **28**, 57.
- Marley, M. C., Richter, S. D., Cody, R. J., and Cliff, B. L. 1990. Modeling for in-situ evaluation of soil properties and engineered vapor extraction system design. **In:** Proc. National Water Well Association/American Petroleum Institute Petroleum Hydrocarbon Conf. Houston, Texas, October 31 to November 2.
- McWhorter, D. B. 1990. Unsteady radial flow of gas in the vadose zone. *J. Contam. Hydrol.* **5**, 297.
- Pedersen, T. A. and Curtis, J. T. 1991. Soil Vapor Extraction Technology: Reference Handbook. EPA/540/2-92/003. Cincinnati, OH, USEPA-RREL.
- Rawlins, S. L. and Campbell, G. S. 1986. Water potential: thermocouple psychrometry, **In:** *Methods of Soil Analysis, Part 1, Physical and Mineralogical Methods*, p. 597. (Klute, A., Ed.) Agron. Monogr. No. 9, 2nd ed. Madison, WI, American Society of Agronomy-Soil Science Society of America.
- Shan, C., Falta, R. W., and Javandel, I. 1992. Analytical solutions for steady state gas flow to a soil vapor extraction well. *Water Resour. Res.* **28(4)**:1105.
- Sleep, B. E. and Sykes, J. F. 1989. Modeling the transport of volatile organics in variably saturated media. *Water Resour. Res.* **25(1)**:81.
- U.S. EPA. 1991. Engineering Bulletin: In Situ Soil Vapor Extraction Treatment. EPA-OERR/ORD, EPA/540/2-91/006.
- Vachaud, G., Vauclin M., and Khanji, D. 1973. Effects of air pressure on water flow in an unsaturated vertical column of sand. *Water Resour. Res.* **9(1)**:160.